APPLIED ORGANOMETALLIC CHEMISTRY
Appl. Organometal. Chem. 2005; **19**: 935–944
Published online in Wiley InterScience (www.interscience.wiley.com). DOI:10.1002/aoc.937

Electrospray ionization mass spectrometry of tributyltin(IV) complexes and their larvicidal activity on mosquito larvae: crystal and molecular structure of polymeric ($Bu_3Sn[O_2CC_6H_4\{N{=}N(C_6H_3\text{-}4\text{-}OH(C(H){=}NC_6H_4OCH_3\text{-}4))\}\text{-}o])_n$

Tushar S. Basu Baul[1]*, Keisham Surjit Singh[1], Michal Holčapek[2], Robert Jirásko[2], Anthony Linden[3], Xueqing Song[4], Alejandra Zapata[4] and George Eng[4]**

[1]Department of Chemistry, North-Eastern Hill University, NEHU Permanent Campus, Umshing, Shillong 793 022, India
[2]University of Pardubice, Faculty of Chemical Technology, Department of Analytical Chemistry, Čs. legií 565, 53210 Pardubice, Czech Republic
[3]Institute of Organic Chemistry, University of Zurich, Winterthurerstrasse 190, CH-8057 Zurich, Switzerland
[4]Department of Chemistry and Physics, University of the District of Columbia, Washington, DC 20008, USA

Received 16 December 2004; Revised 1 April 2005; Accepted 4 April 2005

A series of tributyltin(IV) complexes of 2-[(*E*)-2-(3-formyl-4-hydroxyphenyl)-1-diazenyl]benzoic acid and 4-[((*E*)-1-{2-hydroxy-5-[(*E*)-2-(2-carboxyphenyl)-1-diazenyl]phenyl}methylidene)amino]aryls have been investigated by electrospray mass spectrometry (ESI-MS) and tandem mass spectrometry (MS^n) techniques. The assignments are facilitated by agreement between observed and calculated isotopic patterns and MS^n studies. Single-crystal X-ray crystallography of $(Bu_3Sn[O_2CC_6H_4\{N{=}N(C_6H_3\text{-}4\text{-}OH(C(H){=}NC_6H_4OCH_3\text{-}4))\}\text{-}o])_n$ reveals a polymeric structure. Toxicity studies of the tributyltin(IV) complexes of the 4-[((*E*)-1-{2-hydroxy-5-[(*E*)-2-(2-carboxyphenyl)-1-diazenyl]phenyl}methylidene)amino]aryls on the second larval instar of the *Aedes aegypti* and *Anopheles stephensi* mosquito larvae are also reported. The LC_{50} values indicate that the complexes are effective larvicides, which range from a low of 0.36 ppm to a high of 0.69 ppm against the *Ae. aegypti* larvae and between 0.82 and 1.17 ppm against the *An. stephens*i larvae. Copyright © 2005 John Wiley & Sons, Ltd.

KEYWORDS: organotin; tributyltins; carboxylates; 2-[(*E*)-2-(3-formyl-4-hydroxyphenyl)-1-diazenyl]benzoic acid; 4-[((*E*)-1-{2-hydroxy-5-[(*E*)-2-(2-carboxyphenyl)-1-diazenyl]phenyl}methylidene)amino]aryls; ESI-MS; X-ray; *Aedes aegypti*; *Anopheles stephensi*; mosquito; larvae

*Correspondence to: Tushar S. Basu Baul, Department of Chemistry, North-Eastern Hill University, NEHU Permanent Campus, Umshing, Shillong 793 022, India.
E-mail: basubaul@hotmail.com
**Correspondence to: Anthony Linden, Institute of Organic Chemistry, University of Zurich, Winterthurerstrasse 190, CH-8057 Zurich, Switzerland.
E-mail: alinden@oci.unizh.ch

Contract/grant sponsor: Department of Science & Technology, New Delhi, India; Contract/grant number: SP/S1/F26/99.
Contract/grant sponsor: National Institutes of Health Minority Biomedical Research Support Program, USA; Contract/grant number: GM08005.
Contract/grant sponsor: The Grant Agency of the Czech Republic; Contract/grant number: 203/03/1071.

INTRODUCTION

Organotin compounds are currently one of the most studied organometallic systems in terms of industrial and agricultural applications, which involve such widely divergent fields as stabilizers for poly(vinylchloride), industrial catalysts and agricultural agents.[1–3] In addition, tributyltin compounds display a large array of biocidal properties and are used in wood preservatives and in marine antifouling paints.[4] Owing to their wide range of biocidal activities, triorganotins have also been screened as possible larvicides against various species of mosquito.[5,6] For example, tributyltin complexes were screened against the fourth larval instar stage of the *Aedes aegypti* mosquito and were found to be more effective than the triphenyltin derivatives.[7] Consequently, a series of azo-butyltin compounds, viz. tributyltin 5-[(*E*)-2-(aryl)-1-diazenyl]-2-hydroxybenzoates and tributyltin 2-[(*E*)-2-(3-formyl-4-hydroxyphenyl)-1-diazenyl]benzoate have been investigated and have shown moderate[8] and better[9] activities respectively. In view of the overall effectiveness of the tributyltins, and in search of better candidates for the control of various mosquito larvae, the present investigation evaluates the toxicity of a series of tributyltin azo-Schiff base complexes derived from 4-[((*E*)-1-{2-hydroxy-5-[(*E*)-2-(2-carboxyphenyl)-1-diazenyl]phenyl}methylidene)amino]aryls against the *Ae. aegypti* and *An. stephensi* mosquito larvae. These two species of mosquito are responsible for the transmission of yellow fever and malaria respectively.

The preparation of the ligands L^1HH' (Fig. 1) and $L^{2-5}HH'$ (Fig. 2) and their tributyltin complexes, Bu_3SnL^1H (**1**), Bu_3SnL^2H (**2**), Bu_3SnL^3H (**3**), Bu_3SnL^4H (**4**) and Bu_3SnL^5H (**5**), has been described in an earlier report,[9] along with the characterization of the compounds by carbon, hydrogen and nitrogen analyses, IR, ^1H, ^{13}C and ^{119}Sn NMR, and ^{119}Sn Mössbauer spectroscopy. The crystal structures of complexes **1** and **4** were also reported,[9] and together with the ^{119}Sn Mössbauer data revealed that the tributyltin complexes form single-stranded polymeric structures, in which the carboxylate oxygen atoms of each aryl ligand bridge two tin atoms and the tin atoms have a slightly distorted trigonal bipyramidal coordination geometry.

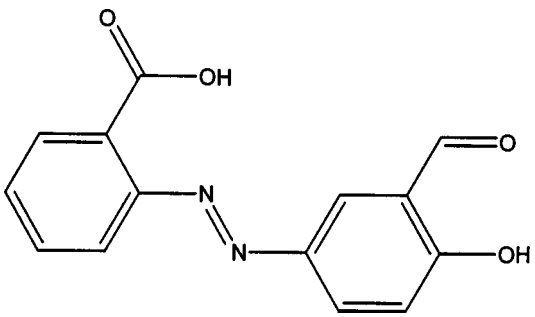

Figure 1. Generic structure of the ligand L^1HH', where H and H′ represent hydroxyl and carboxyl protons respectively.

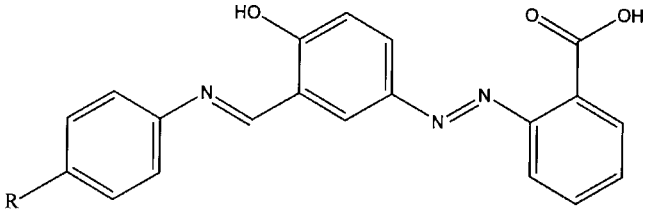

Figure 2. Generic structure of the ligand. L^2HH': R = CH_3; L^3HH:R Br, L^4HH:R Cl; L^5HH:R OCH_3, where H and H′ represent hydroxyl and carboxyl protons respectively.

In addition to the results of the toxicity studies, the current report now extends the previous work by describing the crystal structure of complex **5** and the results of an investigation by electrospray ionization mass spectrometry (ESI-MS). Before the advent of ESI-MS, conventional electron ionization (EI) was the only choice for the mass spectrometric analysis of organotin compounds. Unfortunately, EI can be used only for compounds with sufficient volatility and the compounds analysed undergo significant fragmentation, frequently leading to the absence of molecular ions, which is very important for the spectra interpretation. EI was restricted to similar species, such as tributyltin, triphenyltin and so on.[10,11] ESI-MS makes possible the analysis of non-volatile compounds from medium polarity to ionic species, including the organometallic compounds.[12,13] It was shown in previous studies of our group[14–17] and others[18–20] that the combination of the positive- and negative-ion ESI spectra together with tandem mass spectrometric (MS^n) experiments on the ions of interest can yield valuable information for the structure characterization. The presence of unexpected adducts in mass spectra for tributyltin complexes have already been reported.[20] The novelty of this work is the measurement of polymeric tributyltin compounds with m/z values higher than m/z 1000 or even 1500 followed by detailed MS^n studies of observed fragment ions.

EXPERIMENTAL

Materials

Compounds **1**–**5** were prepared as described earlier.[9]

Mass spectrometry

Positive-ion and negative-ion ESI mass spectra were measured on an ion trap analyser (Esquire 3000, Bruker Daltonics, Bremen, Germany) in the range m/z 50–2000. The samples were dissolved in 100% acetonitrile (HPLC grade, Merck) and analysed by direct infusion at a flow rate of 5 μl min^{-1}. The selected precursor ions were further analysed by MS–MS analyses under the following conditions: isolation width $m/z = 8$ for ions containing one tin atom and $m/z = 12$ for ions containing more tin atoms; collision amplitude in the range 0.7–1.0 V, depending on the precursor ion stability; ion source

Table 1. Ions observed in the first-order and MS–MS using ESI both in positive-ion and negative-ion modes for compound **1**

m/z		Summary formula	Relative abundance (%)	Observed ions in MS–MS spectra[a,b]
Positive ions				
1739	$[2 \times M + 2 \times SnBu_3 - 2 \times H + K]^+$	$C_{76}H_{124}N_4O_8Sn_4K$	1	889
1723	$[2 \times M + Na - 2 \times H + 2 \times SnBu_3]^+$	$C_{76}H_{124}N_4O_8Sn_4Na$	4	873
1449	$[2 \times M + K - H + SnBu_3]^+$	$C_{64}H_{98}N_4O_8Sn_3K$	2	889; 599; 583
1433	$[2 \times M + Na - H + SnBu_3]^+$	$C_{64}H_{98}N_4O_8Sn_3Na$	17	873; 583
1159	$[2 \times M + K]^+$	$C_{52}H_{72}N_4O_8Sn_2K$	3	889; 599
1143	$[2 \times M + Na]^+$	$C_{52}H_{72}N_4O_8Sn_2Na$	27	873; 583
963	$[2 \times M - butene - CO_2 - Bu]^+$	$C_{43}H_{55}N_4O_6Sn_2$	9	583; 403
889	$[M + K - H + SnBu_3]^+$	$C_{38}H_{62}N_2O_4Sn_2K$	11	—[d]
873	$[M + Na - H + SnBu_3]^+$	$C_{38}H_{62}N_2O_4Sn_2Na$	10	—[d]
851	$[M + SnBu_3]^+$	$C_{38}H_{63}N_2O_4Sn_2$	46	793; 583; 525; 503; 485; 459; 373; 345; 253
599	$[M + K]^+$	$C_{26}H_{36}N_2O_4SnK$	39	291; 177
583	$[M + Na]^+$	$C_{26}H_{36}N_2O_4SnNa$	100	275; 234; 177
561	$[M + H]^+$	$C_{26}H_{37}N_2O_4Sn$	21	485; 291
403	$[M - butene - CO_2 - Bu]^+$	$C_{17}H_{19}N_2O_2Sn$	20	345
Negative ions				
1409	$[2 \times M + SnBu_3 - 2 \times H]^-$	$C_{64}H_{97}N_4O_8Sn_3$	3	559; 515
1119	$[2 \times M - H]^-$	$C_{52}H_{71}N_4O_8Sn_2$	2	559
911	$[M - H + HOSnBu_3 + CO_2]^-$	$C_{39}H_{63}N_2O_7Sn_2$	6	559
621	$[M - H + H_2O + CO_2]^-$	$C_{27}H_{37}N_2O_7Sn$	6	559; 269
575[c]	$[M_{carboxyl} - H]^-$	$C_{26}H_{35}N_2O_5Sn$	4	531; 487
559	$[M - H]^-$	$C_{26}H_{35}N_2O_4Sn$	27	515; 401; 344
269	$[M - SnBu_3]^-$	$C_{14}H_9N_2O_4$	100	225
225	$[M - SnBu_3 - CO_2]^-$	$C_{13}H_9N_2O_2$	5	—[d]

[a] Interpretation of observed ions in positive-ion MS–MS: m/z 793 $[M + H + SnBu_3 - butane]^+$; m/z 525 $[M + Na - butane]^+$; m/z 503 $[M + H - butane]^+$; m/z 485 $[M + H - butane - H_2O]^+$; m/z 459 $[M + H - butane - CO_2]^+$; m/z 373 $[M + H - butane - 2 \times butene - H_2O]^+$; m/z 345 $[M + H - 2 \times butane - butene - CO_2]^+$; m/z 291 $[M + K - HOSnBu_3]^+$; m/z 275 $[M + Na - HOSnBu_3]^+$; m/z 253 $[M + H - HOSnBu_3]^+$; m/z 177 $[SnBu]^+$.

[b] Interpretation of observed ions in negative-ion MS–MS: m/z 531 $[M_{carboxyl} - H - CO_2]^-$; m/z 515 $[M - H - CO_2]^-$; m/z 487 $[M_{carboxyl} - H - 2 \times CO_2]^-$; m/z 401 $[M - H - CO_2 - butane - butene]^-$; m/z 344 $[M - CO_2 - 3 \times Bu]^-$.

[c] Aldehyde group is oxidized to carboxyl group.

[d] Not observed.

temperature of 300 °C; tuning parameter compound stability of 100%; flow rate and pressure of nitrogen of 4 l min^{-1} and 10 psi respectively. The ions observed in the first-order and MS^n spectra, both in positive-ion and negative-ion modes, are summarized in Tables 1–5 for compounds **1**–**5** respectively.

X-ray crystallography

Crystals of compound **5** suitable for an X-ray crystal-structure determination were obtained from chloroform–hexane (1 : 1 v/v). All measurements were made at low temperature on a Nonius Kappa-CCD diffractometer[21] with graphite-monochromated Mo Kα radiation ($\lambda = 0.710\,73$ Å) and an Oxford Cryosystems Cryostream 700 cooler. Data reduction was performed with HKL Denzo and Scalepack.[22] The intensities were corrected for Lorentz and polarization effects, and an empirical absorption correction based on the multi-scan method[23] was applied. Equivalent reflections were merged. The data collection and refinement parameters are given in Table 6. The structure of **5** was solved by SHELXS97,[24] which revealed the positions of all non-hydrogen atoms. There are two symmetry-independent repeats of the principal chemical unit in the asymmetric unit of this one-dimensional polymeric structure. The atomic coordinates were tested carefully for a relationship from a higher symmetry space group using the program PLATON,[25] but none could be found. The terminal methyl group of one butyl ligand on one of the unique tin atoms is disordered over two conformations, as are all atoms of one butyl ligand on the other tin atom and one of the methoxy methyl groups; refinement of constrained site occupation factors for the two orientations of these groups yielded values of 0.57(9), 0.659(6) and 0.519(9) respectively, for the major conformations. Similarity and bond-length restraints were applied to the chemically equivalent bond lengths and angles involving disordered carbon atoms, whereas neighbouring atoms within and between each conformation

of the disordered groups were restrained to have similar atomic displacement parameters. The non-hydrogen atoms were refined anisotropically. All of the hydrogen atoms were placed in geometrically calculated positions and refined using a riding model where each hydrogen atom was assigned a fixed isotropic displacement parameter with a value equal to 1.2 U_{eq} of its parent atom (1.5 U_{eq} for the methyl and hydroxy groups). The orientation of the hydroxy O–H vector was optimized to correspond with the direction that would bring the hydrogen atom closest to the nearest hydrogen bond acceptor. Refinement of the structure was carried out on F^2 using full-matrix least-squares procedures, which minimized the function $\Sigma w(F_o^2 - F_c^2)^2$. A correction for secondary extinction was applied. Two reflections, whose intensities were considered to be extreme outliers, were omitted from the final refinement. All calculations were performed using the SHELXL97 program.[26]

Biological tests

Preparation of the organotin stock solution

Stock solutions of the tributyltin compounds **1**–**5** were prepared by dissolving the complexes in 95% ethanol. The dissolution of the organotin compounds in the organic media was to facilitate the dispersion of the compounds in water.

Mosquito larvae

Dried *Ae. aegypti* mosquito eggs and *An. Stephensi* larvae were obtained from the laboratory of Dr Daniel Strickman, Entomology Department at the Walter Reed Army Institute of Research, Washington, DC. *Ae. aegypti* eggs were hatched in a tray of tap water and after 2–3 days the second larval instar stage was attained. The larvae were maintained in an environmental chamber at 27–28 °C with a humidity of 60–90%. The *An. stephensi* larvae were kept in the same environment chamber under the same conditions. Both species of larvae were fed with ground dog food.

Larval toxicity studies

The toxicity studies were performed in 100 mm × 15 mm disposable Petri dishes using 10 larvae in the second instar stage. The *Ae. aegypti* or *An. stephensi* larvae were transferred into the Petri dishes using a 100 µl: micro-pipetter. An additional 15 ml of deionized water was then added. No turbidity was observed upon the addition of the water. Aliquots of the triorganotin solution were then added to the Petri dish containing the larvae, along with deionized water to give the desired concentration of triorganotin. The total assay volume in each case was 20 ml. Both positive and negative controls were used in the assays. The larvae were exposed to the triorganotin compounds for 24 h, and the mortality rates for the mosquito larvae were determined by visual counting. Mosquito larvae that showed a slight reflex to disturbance were considered alive. A minimum of three trials was used for each assay. Probit analyses[27] were used to determine the LC_{50} (concentration at which the test compounds killed 50% of the tested organisms).

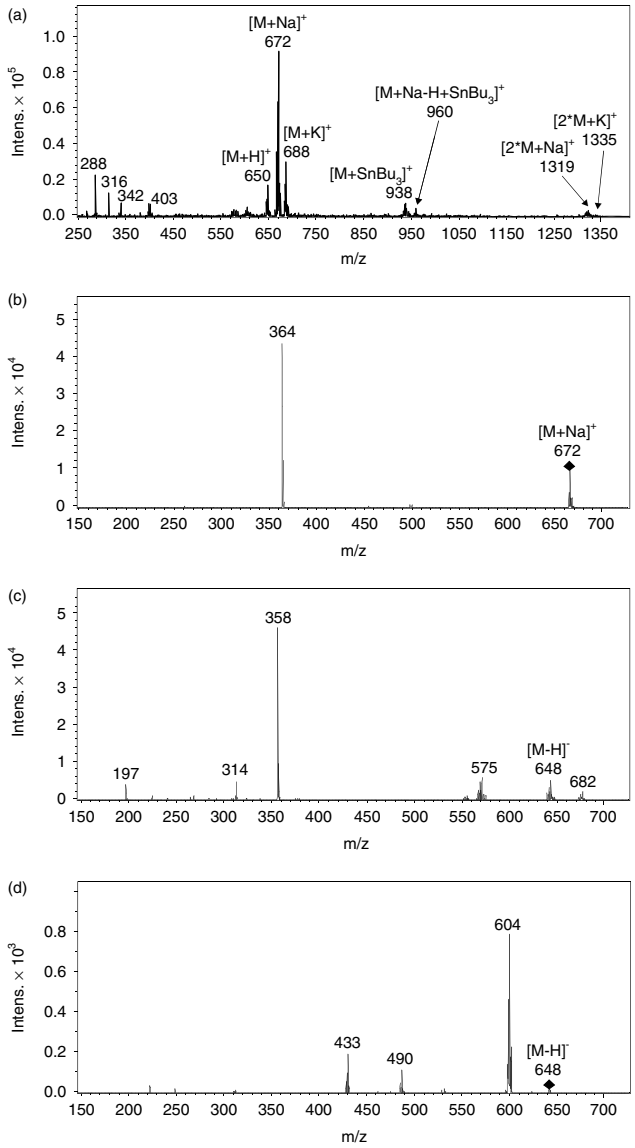

Figure 3. ESI mass spectra of compound **2**: (a) positive-ion first-order spectrum; (b) positive-ion MS–MS of *m/z* 672; (c) negative-ion first-order spectrum; (d) negative-ion MS–MS spectrum of 648.

RESULTS AND DISCUSSION

The synthetic, analytical and spectroscopic data for complexes **1**–**5** were reported in our earlier communication.[9]

ESI mass spectra, both in the positive- and negative-ion modes, were measured using acetonitrile solutions of complexes **1**–**5** and the results are summarized in Tables 1–5. The interpretation of the mass spectra is based on previous studies on ESI-MS measurements of organotin compounds.[14–17] A typical example of an identification approach is illustrated for compound **2** in Fig. 3. In the positive-ion mode (Fig. 3a), the presence of $[M + H]^+$, $[M + Na]^+$ and $[M + K]^+$ enables the unambiguous determination

Table 2. Ions observed in the first-order and MS–MS using electrospray ionization both in positive-ion and negative-ion modes for compound **2**

m/z		Summary formula	Relative abundance (%)	Observed ions in MS–MS spectra[a,b]
Positive ions				
1337	$[2 \times M + K]^+$	$C_{66}H_{86}N_6O_6Sn_2K$	1	978; 688
1321	$[2 \times M + Na]^+$	$C_{66}H_{86}N_6O_6Sn_2Na$	4	962; 672
978	$[M + K - H + SnBu_3]^+$	$C_{45}H_{69}N_3O_3Sn_2K$	1	d
962	$[M + Na - H + SnBu_3]^+$	$C_{45}H_{69}N_3O_3Sn_2Na$	4	808; 790; 656; 570; 458
940	$[M + SnBu_3]^+$	$C_{45}H_{70}N_3O_3Sn_2$	8	610; 592; 574; 548; 534; 478; 462; 434; 406; 342; 298
688	$[M + K]^+$	$C_{33}H_{43}N_3O_3SnK$	33	380
672	$[M + Na]^+$	$C_{33}H_{43}N_3O_3SnNa$	100	500; 364
650	$[M + H]^+$	$C_{33}H_{44}N_3O_3Sn$	19	342; 314; 298; 197
Negative ions				
682	$[M_{2\times OH} - H]^-$	$C_{33}H_{44}N_3O_5Sn$	5	358; 314
648	$[M - H]^-$	$C_{33}H_{42}N_3O_3Sn$	12	604; 490; 433
575	$[Bu_3SnOCOC_6H_4N_2C_6H_3(OH)COO]^-$	$C_{26}H_{35}N_2O_5Sn$	14	—[d]
358	$[M - SnBu_3]^-$	$C_{21}H_{16}N_3O_3$	100	314
314	$[M - SnBu_3 - CO_2]^-$	$C_{20}H_{16}N_3O$	11	209
197	—[c]	$C_{12}H_9N_2O$	9	—[d]

[a] Interpretation of observed ions in positive-ion MS–MS: m/z 808 $[M + Na - H + SnBu_3 - 2 \times butane - butene + H_2O]^+$; m/z 790 $[M + Na - H + SnBu_3 - 2 \times butane - butene]^+$; m/z 656 $[M + Na + SnBu_3 - OSnBu_3]^+$; m/z 610 $[M - Bu + H_2O]^+$; m/z 592 $[M - Bu]^+$; m/z 574 $[M - Bu - H_2O]^+$; m/z 570 $[M + Na - butane - CO_2]^+$; m/z 548 $[M - Bu - CO_2]^+$; m/z 534 $[M - Bu - butane]^+$; m/z 500 $[M + Na - 2 \times butane - butene]^+$; m/z 478 $[M - Bu - butane - butene]^+$; m/z 462 $[M + H - butane - 2 \times butene - H_2O]^+$; m/z 458 $[M + Na - CO_2 - 2 \times butene - butane]^+$; m/z 434 $[M - Bu - butane - butene - CO_2]^+$; m/z 380 $[M + K - HOSnBu_3]^+$; m/z 364 $[M + Na - HOSnBu_3]^+$; m/z 342 $[M + H - HOSnBu_3]^+$; m/z 314 $[M - HOSnBu_3 - CO]^+$; m/z 298 $[M + H - HOSnBu_3 - CO_2]^+$.

[b] Interpretation of observed ions in negative-ion MS–MS: m/z 604 $[M - H - CO_2]^-$; m/z 490 $[M - H - butane - butene - CO_2]^-$; m/z 433 $[M - H - 2 \times butane - butene - CO_2]^{-\cdot}$; m/z 209 $[M - SnBu_3 - CO_2 - N_2 - benzene]^{-\cdot}$.

[c] Not identified.

[d] Not observed.

of the molecular weight (MW) for all compounds studied. The presence or absence of a tin atom in individual ions can easily be recognized on the basis of 10 characteristic natural tin isotopes with the most abundant ^{120}Sn isotope. All m/z values in Tables 1–5 are related to the ^{120}Sn isotope. The low-mass ions at m/z 288 and 316, shown in Fig. 3a, do not contain a tin atom and they belong to background impurities not related to the main compound, as confirmed in the subsequent MS^n experiments, where these ions are missing, e.g. the MS–MS spectrum of m/z 672 (Fig. 3b). The fragment ion $[M + Na - HOSnBu_3]^+$ at m/z 364 is the only ion in the MS–MS spectrum of $[M + Na]^+$. The first-order negative-ion ESI mass spectrum (Fig. 3c) shows the deprotonated molecule $[M - H]^-$ and also some fragment ions (see Table 2 for details). The other neutral logical losses are found in the MS–MS spectrum of $[M - H]^-$ at m/z 648 (Fig. 3d), such as $[M - H - CO_2]^-$ at m/z 604, $[M - H - butane - butene - CO_2]^-$ at m/z 490 and $[M - H - 2 \times butane - butene - CO_2]^-$ at m/z 433. The detailed explanation of all fragment ions identified is given in Tables 1–5 with several common features. The $[M + Na]^+$ ion is the base peak in all first-order positive-ion ESI mass spectra, which makes possible an easy MW determination. In all cases, the less abundant adduct ions with $SnBu_3$ are observed. The $[M - SnBu_3]^-$ ion is the base peak of all first-order negative-ion mass spectra, accompanied by the less abundant $[M - H]^-$ ion. For compounds **1**–**3**, the adduct ion with two hydroxyl groups $[M_{2\times OH} - H]^-$ is observed with a lower relative intensity than the $[M - H]^-$ ion. The other neutral logical losses in the MS^n are butane, butene, CO_2, $HOSnBu_3$, H_2O, etc. The mass spectra of all compounds are in accordance with the suggested structures.

The crystal structure of **5** shows that the compound has a one-dimensional polymeric structure (Fig. 4) very similar to the structures of $(Bu_3Sn[O_2CC_6H_4\{N{=}N(C_6H_3\text{-}4\text{-}OH\text{-}5\text{-}CHO)\}\text{-}o])_n$ (**1**) and $(Bu_3Sn[O_2CC_6H_4\{N{=}N(C_6H_3\text{-}4\text{-}OH(C(H){=}NC_6H_4Cl\text{-}4))\}\text{-}o])_n$ (**4**), which were reported earlier.[9] The asymmetric unit contains two repeats of the principal chemical unit and the structure is built from adjacent $SnBu_3$ moieties bridged by the two carboxylate oxygen atoms of a single aryl ligand, with the pattern then continuing indefinitely, as illustrated in Fig. 5. The two symmetry-independent tin atoms have slightly distorted *trans*-R_3SnO_2 trigonal bipyramidal coordination geometry with equatorial butyl groups and carboxylate oxygen atoms occupying axial positions, the two oxygen atoms being from different

Table 3. Ions observed in the first-order and MS–MS using ESI both in positive-ion and negative-ion modes for compound **3**

m/z		Summary formula	Relative abundance (%)	Observed ions in MS–MS spectra[a,b]
Positive ions				
1465	$[2 \times M + K]^+$	$C_{64}H_{80}N_6O_6Sn_2Br_2K$	0.4	1042; 752
1449	$[2 \times M + Na]^+$	$C_{64}H_{80}N_6O_6Sn_2Br_2Na$	3	1026; 736; 428
1026	$[M + Na - H + SnBu_3]^+$	$C_{44}H_{66}N_3O_3Sn_2BrNa$	4	968; 872; 854; 810; 720; 634; 550; 522
1004	$[M + SnBu_3]^+$	$C_{44}H_{67}N_3O_3Sn_2Br$	6	946; 674; 656; 638; 612; 406
752	$[M + K]^+$	$C_{32}H_{40}N_3O_3SnBrK$	8	—[d]
736	$[M + Na]^+$	$C_{32}H_{40}N_3O_3SnBrNa$	100	520; 428; 298
177	$[SnBu]^+$	C_4H_9Sn	5	—[d]
Negative ions				
746	$[M_{2\times OH} - H]^-$	$C_{32}H_{41}N_3O_5SnBr$	2	422; 378
712	$[M - H]^-$	$C_{32}H_{39}N_3O_3SnBr$	14	668; 554; 497; 417; 298
422	$[M - SnBu_3]^-$	$C_{20}H_{13}N_3O_3Br$	100	378; 273
378	$[M - SnBu_3 - CO_2]^-$	$C_{19}H_{13}N_3OBr$	17	273
197	—[c]	$C_{12}H_9N_2O$	4	—[d]

[a] Interpretation of observed ions in positive-ion tandem mass spectra: *m/z* 1042 $[M + K - H + SnBu_3]^+$; *m/z* 968 $[M + Na - H + SnBu_3 - butane]^+$; *m/z* 946 $[M + SnBu_3 - butane]^+$; *m/z* 872 $[M + Na - H + SnBu_3 - 2 \times butane - butene + H_2O]^+$; *m/z* 854 $[M + Na - H + SnBu_3 - 2 \times butane - butene]^+$; *m/z* 810 $[M + Na - H + SnBu_3 - 2 \times butane - butene - CO_2]^+$; *m/z* 720 $[M + Na + SnBu_3 - OSnBu_3]^+$; *m/z* 674 $[M - Bu + H_2O]^+$; *m/z* 656 $[M - Bu]^+$; *m/z* 638 $[M - Bu - H_2O]^+$; *m/z* 634 $[M + Na - butane - CO_2]^+$; *m/z* 612 $[M - Bu - CO_2]^+$; *m/z* 550 $[M + Na + SnBu_3 - OSnBu_3 - 2 \times butene - butane]^+$; *m/z* 522 $[M + Na - CO_2 - 2 \times butene - butane]^+$; *m/z* 520 $[M + Na - 2 \times butane - butene - CO_2]^+$; *m/z* 428 $[M + Na - HOSnBu_3]^+$; *m/z* 406 $[M + H - HOSnBu_3]^+$.
[b] Interpretation of observed ions in negative-ion tandem mass spectra: *m/z* 668 $[M - H - CO_2]^-$; *m/z* 554 $[M - H - butane - butene - CO_2]^-$; *m/z* 497 $[M - H - 2 \times butane - butene - CO_2]^{-\cdot}$; *m/z* 417 $[M - H - 2 \times butane - butene - HBr - CO_2]^{-\cdot}$; *m/z* 298 $[M - SnBu_3 - HBr - CO_2]^-$; *m/z* 273 $[M - SnBu_3 - CO_2 - N_2 - benzene]^{-\cdot}$.
[c] Not identified.
[d] Not observed.

Table 4. Ions observed in the first-order and MS–MS using ESI both in positive-ion and negative-ion modes for compound **4**

m/z		Summary formula	Relative abundance (%)	Observed ions in MS–MS spectra[a,b]
Positive ions				
1361	$[2 \times M + Na]^+$	$C_{64}H_{80}N_6O_6Sn_2Cl_2Na$	5	982; 692
982	$[M + Na - H + SnBu_3]^+$	$C_{44}H_{66}N_3O_3Sn_2ClNa$	3	828; 810; 766; 676; 590; 504; 478
960	$[M + SnBu_3]^+$	$C_{44}H_{67}N_3O_3Sn_2Cl$	6	630; 612; 594; 568; 498; 482; 454; 426; 362
747	—[c]	—[c]	12	—[d]
708	$[M + K]^+$	$C_{32}H_{40}N_3O_3SnClK$	12	—[d]
692	$[M + Na]^+$	$C_{32}H_{40}N_3O_3SnClNa$	100	384; 310
179	$[H_2SnBu]^+$	$C_4H_{11}Sn$	2	—[d]
Negative ions				
668	$[M - H]^-$	$C_{32}H_{39}N_3O_3SnCl$	54	624; 510; 453; 298
378	$[M - SnBu_3]^-$	$C_{20}H_{13}N_3O_3Cl$	100	334; 229
334	$[M - SnBu_3 - CO_2]^-$	$C_{19}H_{13}N_3OCl$	68	297; 229
197	—[c]	$C_{12}H_9N_2O$	11	—[d]

[a] Interpretation of observed ions in positive-ion MS–MS: *m/z* 828 $[M + Na - H + SnBu_3 - 2 \times butane - butene + H_2O]^+$; *m/z* 810 $[M + Na - H + SnBu_3 - 2 \times butane - butene]^+$; *m/z* 766 $[M + Na - H + SnBu_3 - 2 \times butane - butene - CO_2]^+$; *m/z* 676 $[M + Na + SnBu_3 - OSnBu_3]^+$; *m/z* 630 $[M - Bu + H_2O]^+$; *m/z* 612 $[M - Bu]^+$; *m/z* 594 $[M - Bu - H_2O]^+$; *m/z* 590 $[M + Na - butane - CO_2]^+$; *m/z* 568 $[M - Bu - CO_2]^+$; *m/z* 554 $[M - Bu - butane]^+$; *m/z* 504 $[M + Na + SnBu_3 - OSnBu_3 - 2 \times butane - butene]^+$; *m/z* 498 $[M - Bu - butane - butene]^+$; *m/z* 482 $[M + H - butane - 2 \times butene - H_2O]^+$; *m/z* 478 $[M + Na - 2 \times butene - butane - CO_2]^+$; *m/z* 454 $[M - Bu - butane - butene - CO_2]^+$; *m/z* 400 $[M + K - HOSnBu_3]^+$; *m/z* 384 $[M + Na - HOSnBu_3]^+$; *m/z* 362 $[M + H - HOSnBu_3]^+$.
[b] Interpretation of observed ions in negative-ion MS–MS: *m/z* 624 $[M - H - CO_2]^-$; *m/z* 510 $[M - H - butane - butene - CO_2]^-$; *m/z* 453 $[M - H - 2 \times butane - butene - CO_2]^{-\cdot}$; *m/z* 298 $[M - SnBu_3 - HCl - CO_2]^-$; *m/z* 297; *m/z* 229 $[M - SnBu_3 - CO_2 - N_2 - benzene]^{-\cdot}$.
[c] Not identified.
[d] Not observed.

Table 5. Ions observed in the first-order and MS–MS using ESI both in positive-ion and negative-ion modes for compound **5**

m/z		Summary formula	Relative abundance (%)	Observed ions in MS–MS spectra[a,b]
Positive ions				
1369	$[2 \times M + K]^+$	$C_{66}H_{86}N_6O_8Sn_2K$	1	994; 704
1353	$[2 \times M + Na]^+$	$C_{66}H_{86}N_6O_8Sn_2Na$	4	978; 688; 380
978	$[M + Na - H + SnBu_3]^+$	$C_{45}H_{69}N_3O_4Sn_2Na$	4	920; 824; 806; 762; 672; 586; 500; 472
956	$[M + SnBu_3]^+$	$C_{45}H_{69}N_3O_4Sn_2$	8	626; 608; 590; 564; 550; 478; 450; 422; 358
745	—[c]	—[c]	15	—[d]
704	$[M + K]^+$	$C_{33}H_{43}N_3O_4SnK$	21	—[d]
688	$[M + Na]^+$	$C_{33}H_{43}N_3O_4SnNa$	100	380
666	$[M + H]^+$	$C_{33}H_{44}N_3O_4Sn$	14	358; 330; 314
Negative ions				
664	$[M - H]^-$	$C_{33}H_{42}N_3O_4Sn$	30	620; 506; 449
374	$[M - SnBu_3]^-$	$C_{21}H_{16}N_3O_4$	100	330; 315
330	$[M - SnBu_3 - CO_2]^-$	$C_{20}H_{16}N_3O_2$	9	315
197	—[c]	$C_{12}H_9N_2O$	2	—[d]

[a] Interpretation of observed ions in positive-ion MS–MS: m/z 994 $[M + K - H + SnBu_3]^+$; m/z 920 $[M + Na - H + SnBu_3 - butane]^+$; m/z 824 $[M + Na - H + SnBu_3 - 2 \times butane - butene + H_2O]^+$; m/z 806 $[M + Na - H + SnBu_3 - 2 \times butane - butene]^+$; m/z 762 $[M + Na - H + SnBu_3 - 2 \times butane - butene - CO_2]^+$; m/z 672 $[M + Na + SnBu_3 - OSnBu_3]^+$; m/z 626 $[M - Bu + H_2O]^+$; m/z 608 $[M - Bu]^+$; m/z 590 $[M - Bu - H_2O]^+$; m/z 586 $[M + Na - butane - CO_2]^+$; m/z 564 $[M - Bu - CO_2]^+$; m/z 550 $[M - Bu - butane]^+$; 500 $[M + Na + SnBu_3 - OSnBu_3 - 2 \times butane - butene]^+$; m/z 478 $[M + H - butane - 2 \times butene - H_2O]^+$; m/z 472 $[M + Na - 2 \times butane - butene - CO_2]^+$; m/z 450 $[M - Bu - butane - butene - CO_2]^+$; m/z 380 $[M + Na - HOSnBu_3]^+$; m/z 358 $[M + H - HOSnBu_3]^+$; m/z 330 $[M + H - HSnBu_3 - CO_2]^+$; m/z 314 $[M + H - HOSnBu_3 - CO_2]^+$.
[b] Interpretation of observed ions in negative-ion MS–MS: m/z 620 $[M - H - CO_2]^-$; m/z 506 $[M - H - butane - butene - CO_2]^-$; m/z 449 $[M - H - 2 \times butane - butene - CO_2]^-$; m/z 315 $[M - SnBu_3 - CH_4 - CO_2]^-$.
[c] Not identified.
[d] Not observed.

carboxylate ligands. Selected geometric parameters are given in Table 7. One of the carboxylate oxygen atoms in each aryl ligand (O(1) and O(5)) can be considered to be coordinating asymmetrically to both adjacent tin atoms in the chain, because, in addition to an Sn–O distance of about 2.42 Å, each of these oxygen atoms is also involved in a much longer intrachain Sn···O interaction with a distance of about 3.20 Å. A similar property was observed in the structures of **1** and **4**.[9] Although these long distances are well inside the sum of the van der Waals radii of the tin and oxygen atoms (ca 3.6 Å), there does not appear to be any significant distortion of the trigonal bipyramidal coordination geometry as a result of this contact. Nonetheless, the interaction may be responsible for the observed length of the formal Sn–O bond involving these oxygen atoms, because the Sn–O distances of about 2.42 Å are about 0.2 Å longer that the Sn–O distances involving the carboxylate oxygen atoms (O(2) and O(6)) that do not have an additional Sn···O interaction.

The hydroxy group in each carboxylate ligand of **5** forms an intraligand hydrogen bond with the adjacent imino nitrogen atom. Some of the butyl groups in the structure are disordered, as is common for complexes involving the Bu_3Sn core (see Experimental section). The methoxy methyl group of one of the two symmetry-independent carboxylate ligands is also disordered over two conformations, which differ by an approximately 180° rotation about the C(ring)–O bond.

As with the structures of **1** and **4**,[9] the structure of **5** corresponds with the type **II** polymeric motif described by Willem *et al.*[28] for related R_3SnO_2CR' compounds. As in related structures,[9,28] the polymeric chain in the structure of **5** propagates in a 2_1 screw fashion, although it is a non-crystallographic pseudo-2_1 screw axis on this occasion. The Sn···Sn distances in **5** are 5.3520(3) and 5.3200(3) Å, which agree very well with the mean repeat distance found in other type **II** carboxylate-bridged triorganotin species[9,28,29] and further confirms that the repeat distance is essentially independent of the nature of the tin-bound substituents and carboxylate residues.

The polymeric structures of **1, 4**, and **5** contrast with the ESI-MS data, where the polymeric ions have only low relative abundances in the positive ion ESI-MS and are totally absent in the negative ion ESI-MS, which may be caused by easy fragmentation of polymeric species and decomposition of polymers upon dissolution.

Larval toxicity studies

The LC_{50} values, in parts per million, and their standard deviations for the tributyltin complexes **2**–**5** screened against

Table 6. Crystallographic data and structure refinement parameters for **5**

Empirical formula	$C_{33}H_{43}N_3O_4Sn$
Formula weight	664.32
Crystal size (mm)	0.15 × 0.20 × 0.27
Colour and morphology	Orange, prism
Temperature (K)	160(1)
Crystal system	Triclinic
Space group	$P\bar{1}$
a (Å)	10.2502(2)
b (Å)	13.2405(2)
c (Å)	23.4197(4)
α (°)	88.548(1)
β (°)	86.0704(9)
γ (°)	88.992(1)
V(Å^3)	3169.6(1)
Z	4
D_{calc}(g cm^{-3})	1.392
Linear absorption coefficient (mm^{-1})	0.845
Transmission factors (min, max)	0.739, 0.888
$2\theta_{max}$ (°)	55
Reflections measured	62 292
Independent reflections (R_{int})	14 479 (0.056)
Reflections with $I > 2\sigma(I)$	11 074
No. of parameters	810
No. of restraints	114
$R(F)$ ($I > 2\sigma(I)$ reflns)	0.041
$wR(F^2)$ (all data)	0.088
GOF(F^2)	1.07
Max, min $\Delta\rho$(eÅ^{-3})	1.17, −0.77

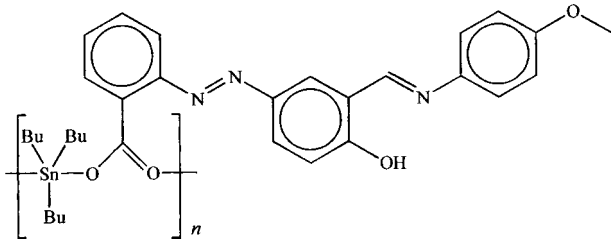

Figure 4. A line diagram showing the polymeric structure of $[Bu_3SnL^5H]_n$ (**5**).

the second larval instar stage of both the *Ae. aegypti* and *An. stephensi* mosquitoes are given in Table 8. The data indicate that the complexes are effective larvicides against these two species of mosquito. They range from a low of 0.36 ppm to a high of 0.69 ppm against the *Ae. aegypti* larvae, and between 0.82 and 1.17 ppm against the *An. stephens*i larvae. The larvicidal activities for the present compounds are similar to those that have been reported in the literature.[7,8,30,31] Furthermore, in general, the larvicidal activities are comparable to or better than the reported results

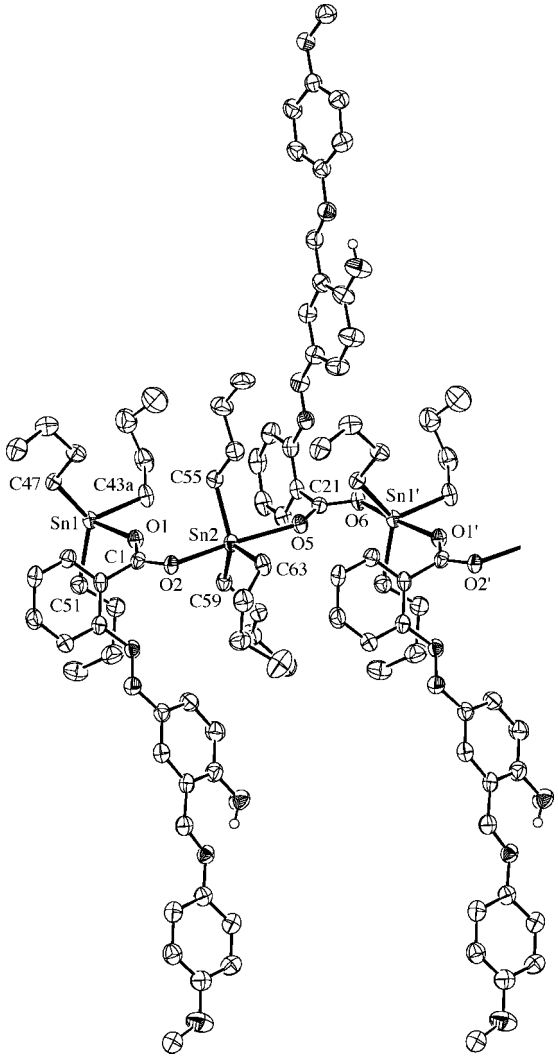

Figure 5. A segment of the polymeric $[Bu_3SnL^5H]_n$ chain in **5** showing the asymmetric unit plus one additional $[Bu_3SnL^5H]$ unit (50% probability ellipsoids; only one of the disordered conformations of the ligands is shown).

for the natural product dioncophylline A, which was tested against the first to the fourth larval states of the *An. stephensi* mosquito.[6] However, these compounds were not as effective as Malathion or Temephos, which were screened against the fourth instar of the *Ae. aegypti*.[5]

A comparison of the two larvae indicates that the *An. stephensi* larvae were more tolerant to the compounds. This finding is in agreement with an earlier study involving the sensitivity of these same two species of larvae towards a series of triorganotin dithiocarbamates.[32] The earlier study reported that, similar to the present study, the *An. stephensi* larvae were more tolerant to the dithiocarbamates than the *Ae. aegypti* larvae. This would further support the view that the same compound may have a different toxicity on different species of mosquito larvae.[32]

Table 7. Selected bond lengths (Å) and angles (°) for **5**[a]

Sn(1)–O(1)	2.425(2)	Sn(2)–O(2)	2.227(2)
Sn(1)–O(6)^{i}	2.218(2)	Sn(2)–O(5)	2.411(2)
Sn(1)···O(5)^{i}	3.172(2)	Sn(2)···O(1)	3.221(2)
Sn(1)–C(43a)	2.150(4)	Sn(2)–C(55)	2.134(3)
Sn(1)–C(43b)	2.149(5)	Sn(2)–C(59)	2.144(3)
Sn(1)–C(47)	2.145(3)	Sn(2)–C(63)	2.155(3)
Sn(1)–C(51)	2.133(3)		
O(1)–Sn(1)–O(6)^{i}	173.89(7)	O(2)–Sn(2)–O(5)	172.93(7)
O(1)–Sn(1)···O(5)^{i}	142.62(6)	O(2)–Sn(2)···O(1)	43.63(7)
O(1)–Sn(1)–C(43a)	83.6(3)	O(2)–Sn(2)–C(55)	95.9(1)
O(1)–Sn(1)–C(43b)	84.8(7)	O(2)–Sn(2)–C(59)	91.8(1)
O(1)–Sn(1)–C(47)	91.1(1)	O(2)–Sn(2)–C(63)	90.2(1)
O(1)–Sn(1)–C(51)	86.0(1)	O(5)–Sn(2)···O(1)	143.43(6)
O(6)^{i}–Sn(1)···O(5)^{i}	44.37(7)	O(5)–Sn(2)–C(55)	88.1(1)
O(6)^{i}–Sn(1)–C(43a)	90.4(3)	O(5)–Sn(2)–C(59)	91.2(1)
O(6)^{i}–Sn(1)–C(43b)	89.1(7)	O(5)–Sn(2)–C(63)	82.8(1)
O(6)^{i}–Sn(1)–C(47)	93.0(1)	C(55)–Sn(2)–C(59)	120.2(1)
O(6)^{i}–Sn(1)–C(51)	95.6(1)	C(55)–Sn(2)–C(63)	117.8(1)
C(43a)–Sn(1)–C(47)	119.4(2)	C(59)–Sn(2)–C(63)	121.5(1)
C(43a)–Sn(1)–C(51)	117.1(2)	C(1)–O(1)···Sn(2)	72.0(2)
C(43b)–Sn(1)–C(47)	127.6(4)	Sn(1)–O(1)···Sn(2)	142.49(8)
C(43b)–Sn(1)–C(51)	109.3(3)	C(21)^{i}–O(5)^{i}···Sn(2)	72.8(2)
C(47)–Sn(1)–C(51)	122.6(1)	Sn(1)^{i}–O(5)^{i}···Sn(2)	144.38(8)

[a] Atom labels with superscript 'i' refer to atoms from the next symmetry-related ligand in the polymeric chain.

Table 8. Toxicity of the ligand and the tributyltin complexes against the second instar larval stage of the *Ae. aegypti* and *An. stephensi* mosquito larvae

	Toxicity (ppm)	
Ligand/compound[a]	*Ae. aegypti*	*An. stephensi*
L^1HH'	>20[9]	>20
1	0.27 ± 0.02[9]	0.47 ± 0.01
2	0.55 ± 0.04	1.17 ± 0.01
3	0.36 ± 0.02	0.82 ± 0.02
4	0.69 ± 0.01	1.10 ± 0.02
5	0.57 ± 0.03	0.88 ± 0.04

[a] Refer to Figs 1 and 2 for the ligand framework (L^1HH' to L^5HH').

A quantitative structure–activity relationship (QSAR) is a useful tool for correlating toxicological activities of molecules to their structures. The development of QSARs between organotin and toxicological activities is not new.[33] For example, QSARs have been developed between several series of triorganotins and their larvicidal activities.[32,34] Attempts to develop QSARs in the present study were not fruitful. The inability to generate acceptable QSARs is most likely due to the fact that the small size of the substituent, compared with the overall size of the ligand, had little influence on various molecular descriptors of the molecule, such as size, shape and surface area. These and other molecular descriptors are typical parameters used in developing QSARs.

Also listed in Table 8 are the LC_{50} values for the precursor tributyltin complex (compound **1**) screened against the *An. stephensi* larvae, as well as the ligand (L^1HH') used in the precursor complex. The previously reported data for the *Ae. aegypti* larvae[9] have also been included for comparison. The data clearly show that the toxicity of the tin complex against the *An. stephensi* larvae is substantially higher than that of the ligand alone, as was previously reported for the *Ae. aegypti* larvae. This result supports the earlier finding that the tributyltin portion of the molecule is responsible for the toxicity of the complex.

In addition, the *An. stephensi* larvae were more tolerant to the precursor complex (**1**) than the *Ae. aegypti.* This is in agreement with the results of the present study. It is further noted that the precursor complex is more toxic to both species of larvae than for the current series of complexes reported. The decrease in activity of the current series of complexes may be due to the increase in size of the ligands, since the precursor ligand is smaller. Smaller complexes may improve the toxicity due to their ability to penetrate the organisms better. This observation would suggest that there is an optimum size needed for maximum toxicity. This finding may give investigators a basis for designing new toxicants against these two species of larva. Although the tributyltin complexes are not as effective as other insecticides, such as

Malathion or Temephos[5], their advantages lie in the fact that triorganotins biodegrade in the environment to a non-toxic species, and there is no reported resistance of this class of compounds towards these two species of mosquito.

Supplementary material

CCDC-257402 contains the supplementary crystallographic data for complex **5**. These data can be obtained free of charge via http://www.ccdc.cam.ac.uk/data_request/cif (or from the Cambridge Crystallographic Data Centre, 12 Union Road, Cambridge CB2 1EZ, UK; fax: +44,1223 336033; e-mail: deposit@ccdc.cam.ac.uk).

Acknowledgements

The financial support of the Department of Science & Technology, New Delhi, India (grant no. SP/S1/F26/99, TSBB), National Institutes of Health Minority Biomedical Research Support Program, USA (grant no. GM08005, GE) and the Grant Agency of the Czech Republic (grant no. 203/03/1071, MH and RJ) is gratefully acknowledged.

REFERENCES

1. Poller RC. *The Chemistry of Organotin Compounds*. Logos Press: London, 1970.
2. Davis AG, Smith PJ. In *Comprehensive Organometallic Chemistry*, vol. 2, Wilkinson G, Stone FGA, Abel EW (eds). Pergamon Press: New York, 1982; 519–627.
3. Evans CJ. In *The Chemistry of Tin*, 2nd edition, Smith PJ (ed.). Blackie: London, 1998; 442–474.
4. De Mora SJ. In *Tributyltin: Case Study of an Environmental Contaminant*, De Mora SJ (ed.). Cambridge University Press: London, 1996; 1–20.
5. François G, Looveren MV, Timperman G, Chimanuka B, Assi LA, Holenz J, Bringmann G. *J. Ethnopharmacol.* 1996; **54**: 125.
6. Kumar Das VG, Kuan LY, Sudderuddin KI, Chang CK, Thomas Y, Yap CK, Lo MK, Hoi-sen Y. *Toxicology* 1984; **32**: 57.
7. Nguyen TT, Ogwuru N, Eng G. *Appl. Organometal. Chem.* 2000; **14**: 345.
8. Basu Baul TS, Dhar S, Rivarola E, Smith FE, Butcher R, Song X, McCain M, Eng G. *Appl. Organometal. Chem.* 2003; **17**: 261.
9. Basu Baul TS, Singh KS, Song X, Zapata A, Eng G, Linden A. *J. Organometal. Chem.* 2004; **689**: 4702.
10. Ostah N, Lawson G. *Appl. Organometal. Chem.* 2000; **14**: 383.
11. Ostah N, Lawson G. *Appl. Organometal. Chem.* 2000; **14**: 874.
12. Gatlin CL, Tureček F. In *Electrospray Ionization Mass Spectrometry*, Cole RB (ed.). Wiley: New York 1997; 527.
13. Traeger JC. *Int. J. Mass Spectrom.* 2005; **200**: 387.
14. Růžička A, Dostál L, Jambor R, Buchta V, Brus J, Císařová I, Holčapek M, Holeček J. *Appl. Organometal. Chem.* 2002; **16**: 315.
15. Jambor R, Dostál L, Růžička A, Císařová I, Brus J, Holčapek M, Holeček J. *Organometallics* 2002; **21**: 3996.
16. Růžička A, Lyčka A, Jambor R, Novák P, Císařová I, Holčapek M, Erben M, Holeček J. *Appl. Organometal. Chem.* 2003; **17**: 168.
17. Kolářová L, Holčapek M, Jambor R, Dostál L, Růžička A, Nádvorník M. *J. Mass Spectrom.* 2004; **39**: 621.
18. Wei J, Miller JM. *J. Mass Spectrom.* 2001; **36**: 806.
19. Armelao L, Schiavon G, Seraglia R, Tondello E, Russo U, Traldi P. *Rapid Commun. Mass Spectrom.* 2001; **15**: 1855.
20. Lawson G, Dahm RH, Ostah N, Woodland ED. *Appl. Organometal. Chem.* 1996; **10**: 125.
21. Hooft R. Kappa—CCD Collect Software. Nonius BV, Delft, The Netherlands, 1999.
22. Otwinowski Z, Minor W. In *Macromolecular Crystallography, Part A*, Carter Jr CW, Sweet RM (eds). *Methods in Enzymology*, vol. 276. Academic Press: New York, 1997; 307–326.
23. Blessing RH. *Acta Crystallogr. Sect A* 1995; **51**: 33.
24. Sheldrick GM. SHELXS97, program for the solution of crystal structures. University of Göttingen, Germany, 1997.
25. Spek AL. PLATON, program for the analysis of molecular geometry. University of Utrecht, The Netherlands, 2004.
26. Sheldrick GM. SHELXL97, program for the refinement of crystal structures. University of Göttingen, Germany, 1997.
27. Finney DJ. *Probit Analysis: A Treatment of the Sigmoid Curve Response*, 3rd edition. Cambridge University Press: London, 1971.
28. Willem R, Verbruggen I, Gielen M, Biesemans M, Mahieu B, Basu Baul TS, Tiekink ERT. *Organometallics* 1998; **17**: 5758.
29. Ng SW, Wei C, Kumar Das VG. *J. Organometal. Chem.* 1988; **345**: 59.
30. Ogwuru N, Duong Q, Song X, Eng G. *Main Group Met. Chem.* 2001; **24**: 775.
31. Eng G, Song X. *Trends Organomet. Chem.* 2002; **4**: 81 and references cited therein.
32. Eng G, Song X, Duong Q, Strickman D, Glass J, May L. *Appl. Organometal. Chem.* 2003; **17**: 218.
33. Craig PJ, Eng G, Jenkins RO. In *Organometallic Compounds in the Environment*, 2nd edition, Craig PJ (ed.). Wiley: New York, 2003; 1–55.
34. Song X, Duong Q, Mitrojorgji E, Zapata A, Nguyen N, Strickman D, Glass J, Eng G. *Appl. Organometal. Chem.* 2004; **18**: 363.

